Journal of Alloys and Compounds 690 (2017) 575–582

Contents lists available at ScienceDirect

Journal of Alloys and Compounds

journal homepage: http://www.elsevier.com/locate/jalcom

Near room temperature magnetocaloric properties and critical behavior of binary Fe_xCu_{100-x}Nanoparticles

D.V.Maheswar Repaka, Vinay Sharma, R.V. Ramanujan*

School of Materials Science and Engineering, Nanyang Technological University, 639798, Singapore

ARTICLE INFO

Article history:
Received 6 April 2016
Received in revised form
16 August 2016
Accepted 17 August 2016
Available online 19 August 2016

Keywords:
Magnetocaloric effect
Fe-based alloys
Critical analysis
Magnetic cooling
Ball milling

ABSTRACT

Low cost, rare earth-free magnetocaloric materials are being intensively studied for near room temperature, energy efficient, "green", magnetic cooling applications. We report the magnetocaloric properties and critical analysis of ball milled Fe_xCu_{100-x} nanoparticles for $x = 30$ to 35. Magnetization measurements of Fe_xCu_{100-x} nanoparticles show soft ferromagnetic behavior at room temperature with small coercivity (H_C) values. The Curie temperature (T_C) could be tuned over a wide temperature range, from 268 K to 360 K, with varying Fe content. The positive slope of the Arrott plots confirms the second order nature of the magnetic transition. Critical analysis of the magnetic phase transition using modified Arrott plots supports the 3D-Heisenberg model. The magnetocaloric effect (MCE) *i.e.,* change in isothermal magnetic entropy (ΔS_m) and relative cooling power (RCP) of Fe_xCu_{100-x} nanoparticles is comparable to that of other Fe based alloys. The high thermal conductivity, soft ferromagnetic behavior and magnetocaloric properties of Fe_xCu_{100-x} nanoparticles are potentially useful for low cost, rare earth element free magnetic cooling applications.

1. Introduction

Magnetic cooling technology relies on the magnetocaloric effect (MCE) is a promising technology for energy efficient, low cost and eco-friendly thermal management systems. Magnetic cooling is a solid state technology which aims to replace low efficiency, environmentally harmful, ozone layer depleting, conventional gas compression based cooling systems [1–4]. The Carnot cycle efficiency of magnetic cooling has already been shown to reach 60%, which is much larger than that of conventional compression based gas refrigerator (less than 40%) [5,6]. BASF, Astronautics Corporation of America and Haier's magnetic cooling wine cooler has been commercialized, then demonstrated that energy efficiency is 35% more than gas compression systems [7]. Following the discovery of the giant magnetocaloric effect in $Gd_5Si_2Ge_2$ [2], investigations of near room temperature magnetocaloric materials have been the subject of intense scientific and industrial interest for magnetic cooling applications. Several prominent magnetocaloric effect (MCE) materials such as Gd [8], Heusler alloys [9,10], and $La(Fe_xSi_{1-x})_{13}$ [11] have been investigated for the past two decades [12]. The magnetocaloric effect (MCE) *i.e.,* the isothermal magnetic entropy change ($-\Delta S_m$) can be calculated using the Maxwell equation $\Delta S_m = \int_0^H \left(\frac{\partial M}{\partial T}\right) dH$. Materials exhibiting a first order magnetic phase transition can show large MCE since $-\Delta S_m$ is proportional to the rate of change of magnetization ($\partial M/\partial T$). However, the thermal and magnetic hysteresis of first order transition materials reduces cooling cycle efficiency. Some rare earth based oxide magnetic materials, *e.g.,* manganites [13–15] also show high isothermal magnetic entropy change near room temperature but the high heat capacity (C (*T*,*H*)) values limit the change in adiabatic temperature, $\Delta T_{ad} = \int_0^H \frac{1}{C(T,H)} \left(\frac{\partial M}{\partial T}\right)_H dH$. Even though the MCE of rare earth based magnetocaloric materials is large, there are several disadvantages including cost, limited supply and the fact that their production is often associated with radioactive mining.

Hence, research has focused on rare earth free magnetic and magnetocaloric materials to reduce cost and develop commercially attractive, environmentally friendly, magnetocaloric materials for magnetic cooling [16–20]. Belyea et al. reported tunable magnetocaloric effect in transition metal based $NiFeCoCrPd_x$ high entropy alloys [21]. Transition metal based Heusler alloys have shown very large magnetocaloric effect at the martensitic phase transition temperature due to the presence of magneto-structural meta-

* Corresponding author.
E-mail address: Ramanujan@ntu.edu.sg (R.V. Ramanujan).

http://dx.doi.org/10.1016/j.jallcom.2016.08.170
0925-8388/

magnetic transitions [22–25]. Magnetic hysteresis and first order magneto-structural transitions result in energy losses, cracks and fatigue which limit the applications of these materials. Rare earth free Fe based soft ferromagnetic metallic alloys are potential candidates for low cost cooling [26]. We have recently reported rare earth free, Fe based, low cost magnetocaloric materials, such as Fe-Ni-B and Fe-Ni-Mn alloys which have very large relative cooling power [27–29]. However, there are very few reports of soft magnetic *binary* metallic alloys with near room temperature magnetic phase transitions.

The Curie temperatures of Fe and Fe based binary soft magnetic alloys ($Ni_{1-x}Fe_x$ and $Co_{1-x}Fe_x$) are typically much higher than room temperature. Tuning of Curie temperature and improving soft ferromagnetic properties for near room temperature applications has been reported [30]. Pure Fe has the bcc structure and a Curie temperature (T_C) of 1043 K. The α-phase *i.e.,* bcc crystal structure alloys exhibit a ferromagnetic transition much higher than room temperature, whereas fcc γ-phase Fe based alloys exhibits a ferromagnetic transition at lower temperatures [31]. Hence, the Fe-Cu alloy system was studied. Fe_xCu_{100-x} binary alloys possess several advantages such as low cost, earth abundance, high thermal conductivity and low heat capacity which are very advantageous for low cost, environmentally friendly magnetic cooling [32]. The immiscible nature of Fe and Cu prevents the formation of Fe-Cu solid-solutions through conventional melting techniques, due to positive heat of mixing [33]. Arc melted alloys and melt spun ribbons exhibit a mix of both bcc and fcc phases [34]. Highly non-equilibrium processing methods, *e.g.,* vapor deposition and sputtering techniques [31,35,36] can form metastable γ-Fe_xCu_{100-x} alloys. Among these techniques, mechanical ball milling can be used to extend the solid miscibility of Fe_xCu_{100-x} alloys over a wide composition range [37,38]. Ball milled Fe_xCu_{100-x}alloys have been reported to crystallize in the fcc crystal structure for compositions $x \leq 60$. They crystallize in a mixture of bcc and fcc for compositions $60 < x < 80$. These alloys crystallize in the bcc crystal structure for compositions $x \geq 80$ [39–42]. The magnetic properties, such as saturation magnetization and coercivity of Fe_xCu_{100-x} alloys strongly depend on grain size and Fe content [43]. These alloys are thermodynamically unstable in bulk form at temperatures greater than 550 K [44–46].

We report the synthesis, structure, magnetic properties, critical analysis and magnetocaloric effect of ball milled Fe_xCu_{100-x}nanoparticles. We investigate the temperature and field dependent magnetic and magnetocaloric properties. The relative cooling power, which is an important parameter for magnetic cooling is also reported. This is the first report of the critical analysis and magnetocaloric effect of these low cost, second order, soft ferromagnetic binary Fe-Cu magnetic nanoparticles for near room temperature magnetic cooling applications.

2. Experimental techniques

Polycrystalline Fe_xCu_{100-x} nanoparticles for $x = 30$, 32, 33 and 35 were prepared by mechanical alloying in Ar atmosphere. The compositions were selected based on a preliminary assessment of T_C values near room temperature. Stoichiometric quantities of high purity Fe (99.99%, Sigma Aldrich) and Cu (99.7%, Sigma Aldrich) powders were mechanically alloyed at 250 rpm for 60 h at room temperature in Ar atmosphere using a Planetary Mill PULVERISETTE-5. The ball to powder mass ratio was maintained at 10:1. The crystal structure and phase were characterized by X-ray diffraction using a Bruker D8 diffractometer with CuK_α radiation ($\lambda = 0.15406$ nm) in the scan range (2θ) from 20 to 90°. The particle size and morphology were determined by transmission electron microscopy (TEM, JEOL 2010) at an operating voltage of 200 kV. The temperature and field dependent magnetic measurements were carried out by Physical Property Measurement Unit (PPMS), (Quantum Design, USA) equipped with a vibrating sample magnetometer (VSM).

2.1. Results and discussion

2.1.1. Structure and phase analysis

Fig 1,(a), (b), (c) and (d) show the XRD patterns of Fe_xCu_{100-x} alloys for $x = 30$, 32, 33 and 35, respectively. Rietveld refinement showed that all samples are single phase with fcc crystal structure and Fm-3m space group. The XRD results confirm the formation of γ-Fe-Cu solid solutions from the immiscible elements. The refined lattice parameters are listed in Table 1. The lattice parameter increases with increasing Fe content from 30 to 33 in Fe_xCu_{100-x}, which is attributed to a magneto-volume effect, where Fe atoms promote repulsion between Cu atoms [37,47]. Fig. 1(e) shows the TEM micrograph and Fig. 1(f) shows the high resolution TEM image for $x = 32$. The inset of Fig. 1(f) shows the selected area diffraction pattern and confirms the fcc crystal structure, with an average spacing between 111 planes of 0.203 nm.

Fig. 2(a), (b), (c) and (d) show the SEM-EDS mapping images of Fe_xCu_{100-x} nanoparticles for $x = 30$, 32, 33 and 35, respectively. These images show the homogeneous distribution of Fe and Cu in the scanned region. The central dark region in $x = 30$ image corresponding to surface irregularities.

Fig. 3(a), (b), (c) and (d) show the particle distribution histograms of Fe_xCu_{100-x} nanoparticles for $x = 30$, 32, 33 and 35, respectively. The average particle size obtained from the particle size distribution curves using TEM micrographs are listed in Table 1. The sample contained small amounts of tungsten carbide impurity which were produced by wear of the ball milling balls. The peaks corresponding to tungsten carbide are denoted by * in XRD

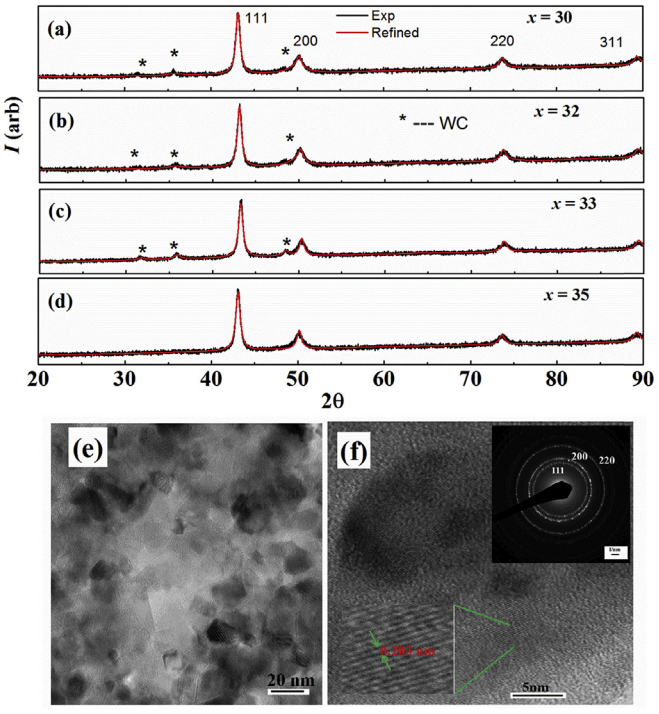

Fig. 1. (a)–(d): XRD patterns of 60 h ball milled Fe_xCu_{100-x} alloys for $x = 30$, 32, 33 and 35. Fig. 1,(e): TEM micrograph of $Fe_{32}Cu_{68}$ nanoparticles. Fig. 1(f): High resolution TEM image of $Fe_{32}Cu_{68}$, inset shows the selected area diffraction pattern of $Fe_{32}Cu_{68}$ nanoparticles. The face centered cubic crystal structure was revealed for all samples.